

Massive-Star Magnetospheres: The Interplay between Outflows, Rotation and Magnetic Fields

Rich Townsend

Department of Astronomy, University of Wisconsin-Madison, 2535 Sterling Hall, 475 N Charter Street, Madison, WI 53706, USA

Abstract. Some massive stars harbor circumstellar environments in which plasma is channeled and confined by a magnetic field. These *massive-star magnetospheres* were first observed over three decades ago, but it is only in the past decade that quantitative models have begun to emerge. This contribution presents an review of these models, highlighting how the distribution of plasma throughout a magnetosphere is sculpted by the interplay between the wind outflow, the centrifugal force due to rotation and the magnetic field.

1. Historical Perspective

In one of those interesting little twists of fate, the first discovery of a massive-star magnetosphere — that is, a circumstellar region where plasma is channeled and confined by the star's magnetic field — actually predates the first field detection. Using photographic-plate spectroscopy, Walborn (1973, 1974) found not only that the Helium-strong B2p star σ Ori E shows the twin-peaked $H\alpha$ emission signifying rotating circumstellar plasma, but also that this emission is variable over a timescale of hours. The novelty of his discovery was not lost on Walborn; his 1974 paper is titled *A New Phenomenon in the Spectrum of Sigma Orionis E*.

Follow-up observations by a number of authors revealed that σ Ori E and a number of other He-strong stars additionally exhibit variations in absorption-line equivalent widths (e.g., Hunger 1974; Pedersen & Thomsen 1977), Balmer shell features (e.g., Groote & Hunger 1976) and photometric indices (e.g., Hesser et al. 1977); moreover, *all* variations appear to be strictly periodic. Then, perhaps cementing its status as a Rosetta Stone, σ Ori E finally revealed the mechanism behind the puzzling variability of the He-strong stars: *magnetic fields*. A ~ 10 kG (polar-strength) dipole magnetic field was detected in σ Ori E by Landstreet & Borra (1978), using photopolarimetry in the wings of $H\beta$. I believe that paper makes the first mention of a 'magnetosphere' in the context of massive stars.

Subsequent photopolarimetric observations of other He-strong stars strongly suggested that magnetic fields are ubiquitous in the class as a whole. Out of a sample of 9 stars, Borra & Landstreet (1979) found 6 to exhibit strong ($\gtrsim 1$ kG), ordered magnetic fields. Similarly, out of a sample of 11 He-strong stars Bohlender et al. (1987) found 9 to be strongly magnetic (of these 9, two were new discoveries, and the remainder follow-ups). Parallel studies of the cooler, later-B type He-weak stars also revealed a high field incidence (e.g., Borra et al. 1983), although the fields are not quite as common — or as strong — as in the He-strong stars.

After this initial golden decade of discovering magnetic fields in the He-peculiar stars (i.e., both He-strong and He-weak objects), further observational progress slowed down considerably, perhaps due to the inherent sensitivity limitations of photopolarimetry. However, on the theoretical side efforts continued to uncover the physical basis for the magnetospheres around these stars, as revealed by twin-peaked $H\alpha$ emission (e.g., σ Ori E; δ Ori C — Bohlender et al. 1991) and/or periodic variations in UV (wind-formed) absorption lines (e.g., HD 37017, HD 64740 — Shore & Brown 1990; HD 5737, HD 79158 — Shore et al. 1990). *Where does the magnetospheric plasma come from — and how does it remain supported above the stellar surface over significant timescales?* Although empirically derived cartoon models proliferated (e.g., Groote & Hunger 1982; Shore & Brown 1990), the real breakthrough was made by Nakajima (1985), who presented the first quantitative treatment to address the issue of magnetospheric support. More on this in §3.

Toward the end of the 1990s the advent of high-resolution spectropolarimeters revived interest in magnetic massive stars by revealing fields in objects *other* than the usual He-peculiar stars. Highlights include the discovery of a field in θ^1 Ori C, the first magnetic O-type star (Donati et al. 2002); the mapping of the complex field topology of the enigmatic B0 star τ Sco (Donati et al. 2006); the detection of a dipole field in the archetypal pulsator β Cephei (Henrichs et al. 2000); and a rapid growth in the number of known-magnetic O- and B-type stars, due most recently to the success of the MiMeS project (see contributions by Gregg Wade and Evelyne Alecian, these proceedings).

Corresponding theoretical progress over the past decade has been driven by numerical magnetohydrodynamical (MHD) simulations, pioneered originally by ud-Doula & Owocki (2002) and Owocki & ud-Doula (2004). These simulations confirm the *magnetically confined wind shock* MCWS paradigm advanced by Babel & Montmerle (1997a,b), which argues that the X-ray emission from stars like θ^1 Ori C arises in the shocks formed when wind streams channeled along closed magnetic loops collide with each other. (Note that the MCWS model was proposed *before* a field was detected in θ^1 Ori C — theory at its finest!). Arguably, however, the key outcome from the work by ud-Doula & Owocki (2002) was something else — the formulation of the *stellar magnetic confinement parameter* η_* .

2. The η_* -W Plane

The magnetic confinement parameter η is defined as the local ratio between magnetic and wind kinetic energy densities,

$$\eta = \frac{B^2/8\pi}{\rho v^2/2} \quad (1)$$

(here, B is the field strength, ρ the plasma density and v the plasma velocity). At each point in a magnetized wind, the magnitude of this parameter determines whether the field channels and controls the wind ($\eta \gg 1$), or whether the wind dominates the field and stretches it out into open, radial configurations ($\eta \ll 1$). ud-Doula & Owocki (2002) demonstrated that for a q -pole global field topology ($q = 2$ for dipole, $q = 3$ for quadrupole, etc.), the functional form of η far from the star can be approximated by

$$\eta \approx \eta_* \left(\frac{r}{R_*} \right)^{-2q}. \quad (2)$$

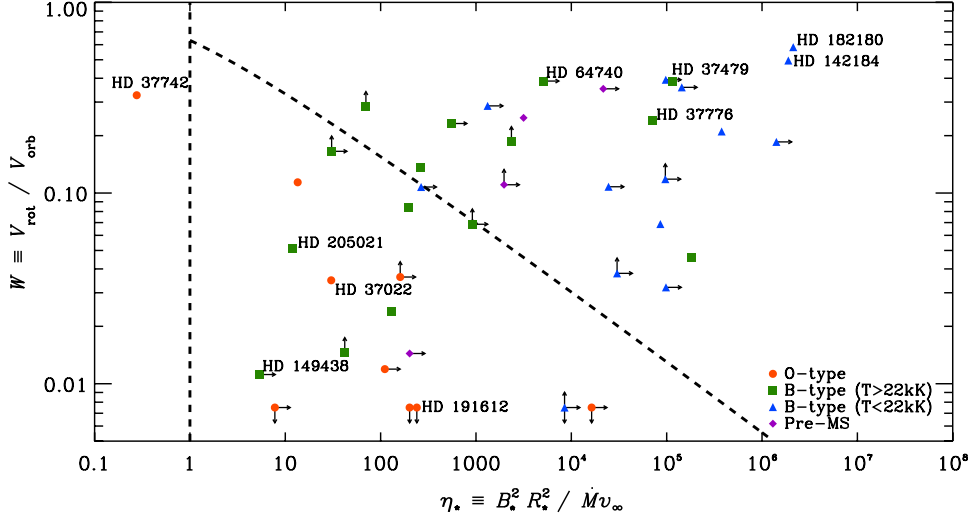


Figure 1. The η_* - W plane for selected magnetic massive stars, colored according to their class. The dashed lines separate the various types of magnetosphere: no magnetosphere ($\eta_* < 1$), dynamical magnetosphere ($\eta_* > 1$, $W \lesssim \eta_*^{-3/8}$) and centrifugal magnetosphere ($\eta_* > 1$, $W \gtrsim \eta_*^{-3/8}$). Telephone directory: HD 37022 = θ^1 Ori C; HD 37479 = σ Ori E; HD 37742 = ζ Ori A; HD 142184 = HR 5907; HD 182180 = HR 7355. Figure courtesy of Véronique Petit.

Here,

$$\eta_* \equiv \frac{B_*^2 R_*^2}{\dot{M} v_\infty} \quad (3)$$

is the *stellar* magnetic confinement parameter, which sets the overall scaling of η in terms of the stellar field strength B_* , radius R_* , wind mass-loss rate \dot{M} and terminal velocity v_∞ .

At the broadest level η_* determines the global configuration of a magnetosphere. Stars with $\eta_* < 1$ (e.g., ζ Ori A; Bouret et al. 2008) cannot maintain closed magnetic loops because $\eta \leq \eta_* < 1$ everywhere, and therefore lack the typical observational signatures (H α emission; UV line variability; X-ray emission from MCWS; etc.) of a magnetosphere. Stars with $\eta_* > 1$, however, will always harbor some kind of magnetosphere extending from the surface out to the Alfvén radius

$$R_A \approx R_* \eta_*^{\frac{1}{2q}} \quad (4)$$

at which $\eta \approx 1$. Inside R_A field lines (typically) remain closed, while outside R_A the wind opens them up.

Nevertheless, this isn't the whole story. A star with $\eta_* > 1$ has answered the first question of how a magnetosphere forms, *where does the magnetospheric plasma come from?* But the second question — *how does it remain supported above the stellar surface over significant timescales?* — still needs to be addressed. In some cases, a valid answer might be *not at all*; even without a putative outward force suspending it near the tops of closed magnetic loops, the plasma will typically take a wind flow time $t_{\text{wind}} \sim R_*/v_\infty$ to fall back to the stellar surface. With a sufficiently high wind mass-loss

rate, the instantaneous mass

$$M_{\text{DM}} \sim \dot{M} t_{\text{wind}} \sim \frac{\dot{M} R_*}{v_{\infty}} \quad (5)$$

contained within this *dynamical magnetosphere* (DM) will be large enough to exhibit an observational signature. Sundqvist et al. (2012) demonstrate that the varying H α emission reported in the slowly rotating (538-day period) magnetic O-star HD 191612 (Wade et al. 2011) is consistent with plasma trapped in a DM (see also Jon Sundqvist’s contribution, these proceedings); for this star $M_{\text{DM}} \sim 2 \times 10^{-10} M_{\odot}$, which is certainly sufficient material to explain the H α emission levels.

The same cannot be said of other stars, however. For σ Ori E, $M_{\text{DM}} \sim 2 \times 10^{-13} M_{\odot}$ (using stellar parameters from Krtićka et al. 2006), which is a couple of orders of magnitude smaller than the $\sim 10^{-11} M_{\odot}$ inferred from observations of the star’s magnetosphere. In this and other He-peculiar stars, the mass-loss rate is simply too small for any appreciable kind of DM to form; therefore, there must be some additional agent at work allowing wind plasma to accumulate over timescales much longer than t_{wind} . This agent is the centrifugal force arising from enforced co-rotation. For plasma situated outside the Kepler radius

$$R_K = W^{-2/3} R_*, \quad (6)$$

where $W \equiv V_{\text{rot}}/V_{\text{orb}}$ is the ratio between the stellar equatorial rotation and orbital velocities, the centrifugal force exceeds the inward pull of gravity and can support plasma near the tops of closed field loops over long time periods. Of course, for such a *centrifugal magnetosphere* (CM) to form it is necessary that R_K exceed the Alfvén radius R_A .

To sum up, three possible scenarios can be identified *vis-a-vis* the formation of a magnetosphere. For $\eta_* < 1$, no magnetosphere is possible. For $\eta_* > 1$ but $R_A < R_K$ a dynamical magnetosphere can form (although its observability depends on \dot{M}); and for $\eta_* > 1$ and $R_A > R_K$ a centrifugal magnetosphere can form. Fig. 1 illustrates these three scenarios in the η_* - W plane, placing many of the stars mentioned in the foregoing discussion in their appropriate locations. Note in particular how the B-type stars (being mostly He-peculiar stars) are generally located in the CM domain, while the O-type stars fall in the DM domain. This is because the B-type stars typically have very large confinement parameters (due to their low mass-loss rates) and can thus more easily satisfy the $R_K > R_*$ requirement for a CM to form; whereas the O-type stars have sufficiently high mass-loss rates that a detectable DM can form.

Not surprisingly, the techniques and tools required to model massive-star magnetospheres depends on the host star’s location in the η_* - W plane. In the DM domain, MHD simulation is the preferred technique (although the RFHD approach described in §3.4 can also be useful). In the CM domain, for sufficiently strong fields, MHD becomes too computationally expensive due to the growing Alfvén speed and shortening Courant timestep. However, in this same limit rigid-field models become applicable.

3. Rigid-Field Models

3.1. Background

Rigid-field models are a class of simplified magnetosphere treatments that assume an arbitrarily strong field, corresponding to the limit $\eta_* \rightarrow \infty$. Within the rigid-field *ansatz*,

the field topology becomes decoupled from the other MHD equations, and can be imposed by fiat as an internal boundary condition. Michel & Sturrock (1974) developed the first rigid-field model, not for a star but for the Io plasma torus in the Jovian magnetosphere. They showed that at radii $r \gtrsim R_K$, the interplay between centrifugal, magnetic and gravitational forces produces loci where plasma from Io's volcanic eruptions can sit in magnetohydrostatic equilibrium.

Nakajima (1985) applied a similar approach to σ Ori E, to develop the first physically realistic model of the star's magnetosphere. In brief, the equation of motion for plasma flowing along a rigid field line is, in the frame co-rotating with angular frequency Ω ,

$$\frac{\partial v}{\partial t} + v \frac{\partial v}{\partial s} + \frac{1}{\rho} \frac{\partial p}{\partial s} = -\frac{d\Phi_{\text{eff}}}{ds}. \quad (7)$$

Here, p is the gas pressure, s is the arc coordinate along the field line, and

$$\Phi_{\text{eff}} = -\frac{GM}{r} - \frac{1}{2}\Omega^2 r^2 \sin^2 \theta \quad (8)$$

is the effective (gravitational plus centrifugal) potential expressed in a spherical coordinate system (r, θ, ϕ) aligned with the rotation axis. In static equilibrium, the equation of motion becomes

$$\frac{1}{\rho} \frac{dp}{ds} = -\frac{d\Phi_{\text{eff}}}{ds}; \quad (9)$$

assuming an isothermal equation of state $p = a^2 \rho$ with sound speed a , solutions take the form

$$\rho(s) = \rho_0 \exp(-\Phi_{\text{eff}}/a^2) \quad (10)$$

where ρ_0 is a normalizing constant proportional to the total amount of mass on the field line. The density is sharply peaked where Φ_{eff} is at its most negative — i.e., at local minima of the effective potential as sampled along the field line, representing points of stable equilibrium.

Nakajima (1985) explored the loci formed by these equilibrium points, finding them to be warped, disk-like surfaces; however, he was constrained by the limited computational resources available at the time. With the advent of cheap computing Preuss et al. (2004) revisited the problem, mapping out the equilibrium surfaces in detail using an alternative (but entirely equivalent) force-balance approach.

3.2. The Rigidly-Rotating Magnetosphere Model

A fundamental limitation of the Nakajima (1985) and Preuss et al. (2004) treatments is their inability to predict the distribution of plasma across the equilibrium surfaces. Although these indicate where plasma will tend to settle, they cannot apply eqn. (10) quantitatively because they lack a prescription for the normalizing density ρ_0 . Townsend & Owocki (2005) addressed this problem in their *rigidly rotating magnetosphere* (RRM) model, which augments the Nakajima (1985) model with an expression for the wind mass flux onto each footpoint of a closed magnetic loop:

$$\dot{m} = \frac{\dot{M}}{4\pi R_*^2} \mu_B, \quad (11)$$

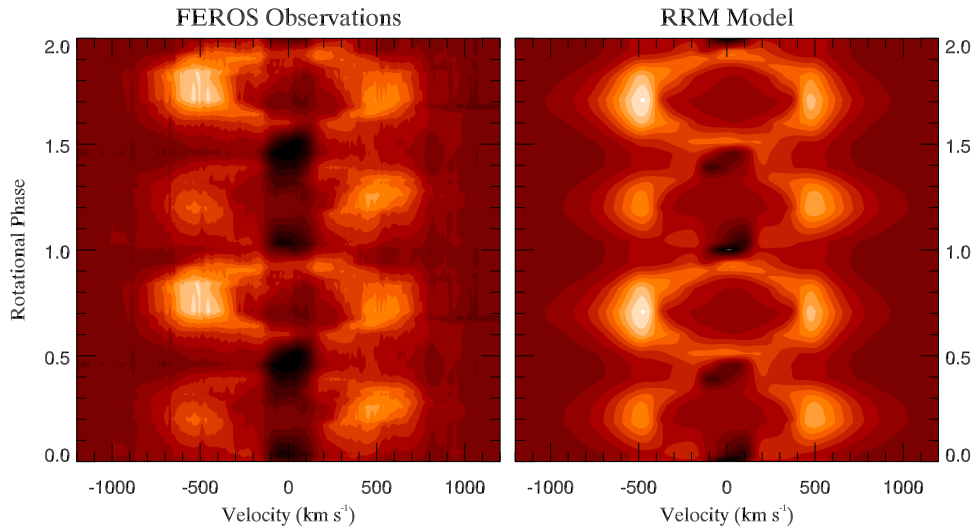


Figure 2. Dynamical $H\alpha$ spectrum of σ Ori E, as observed using the FEROS echelle spectrograph (left) and as predicted by the RRM model (right). White indicates $\sim 15\%$ emission, and black $\sim 5\%$ absorption, relative to the mean photospheric profile. Adapted from Townsend et al. (2005).

where \dot{M} should now be interpreted as the mass-loss rate of the star if it had no field (e.g., as predicted by the Castor et al. 1975, formalism), and μ_B is the projection cosine between the field vector and the stellar surface normal at the footpoint. This expression is based on the scalings found in full MHD simulations by Owocki & ud-Doula (2004); with the ansatz that $\rho_0 \propto \dot{m}$, the magnitude of ρ_0 on each field line is determined (modulo some overall normalization which sets the *total* magnetospheric mass). Then, eqn. (10) gives the relative distribution of mass throughout the entire three-dimensional magnetosphere. Fig. 2 illustrates results from an application of the RRM model to σ Ori E, in order to predict (quite successfully) the time variation of the star’s $H\alpha$ emission.

3.3. Arbitrary-Field RRM Models

A strength of rigid-field approaches is their applicability to arbitrary magnetic topologies — not just to the simple case of an oblique dipole. Fig. 3 illustrates the magnetospheric plasma distribution of HD 37776 (Landstreet’s star) predicted by a new arbitrary-field RRM (A-RRM) code. The circumstellar magnetic field is extrapolated from the surface field maps measured using magnetic Doppler imaging (MDI) by Kochukhov et al. (2011). The basis of the extrapolation process is the recognition that the rigid field *ansatz* is equivalent to assuming a ‘force-free’ field — one in which the Lorentz force $\mathbf{J} \times \mathbf{B}$ completely dominates the other terms in the fluid momentum equation, and therefore must itself be very close to zero if the equation is to be satisfied. This implies that the current density \mathbf{J} is either everywhere parallel to \mathbf{B} , or vanishes completely. The latter scenario is the simplest case to treat, because $\nabla \times \mathbf{B} = \mathbf{J} = 0$ and so the field is derived from a scalar potential,

$$\mathbf{B} = -\nabla\Phi_B. \quad (12)$$

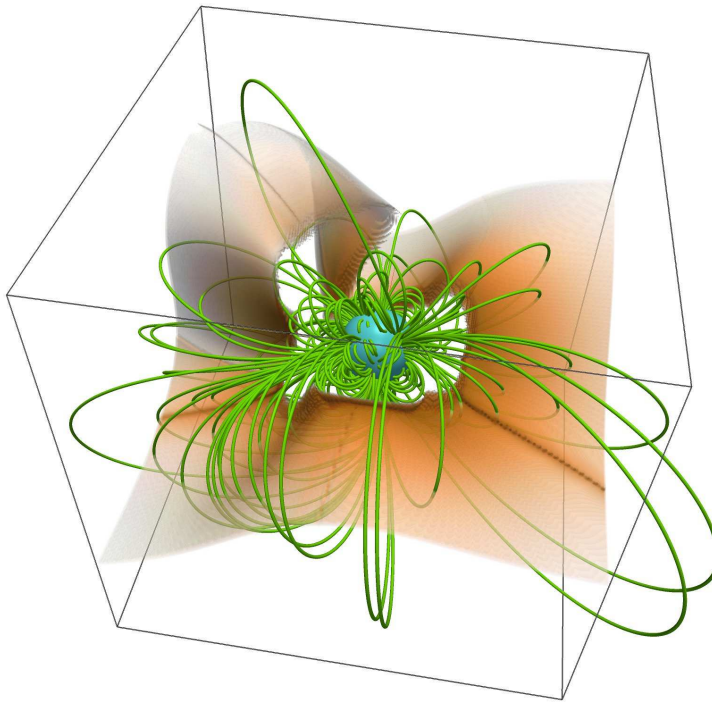


Figure 3. Rendering of an A-RRM simulation of the complex magnetosphere of HD 37776. The plasma density is shown in red/orange, with darker colors corresponding to more-density regions. Selected field lines are plotted in green, and the central star is shown in blue.

Because $\nabla \cdot \mathbf{B} = 0$, the field potential Φ_B must satisfy Laplace's equation. With the boundary condition that the radial field B_r matches the MDI measurements at the stellar surface, Φ_B is completely determined, and so therefore is \mathbf{B} .

This potential-based approach is used to construct the field shown in Fig. 3. The field extrapolation is the computationally expensive part of an A-RRM model; the subsequent calculation of the magnetospheric plasma distribution is relatively straightforward, in that exactly the same formalism (cf. eqns. 10 and 11) as in the RRM model applies.

3.4. The Rigid-Field Hydrodynamics Approach

The focus of the RRM and A-RRM models is on the cool, dense, near-stationary plasma in the magnetosphere — the end product of the MCWS processes in which the wind streams from opposing footpoints collide, are shock-heated to millions of Kelvin, and then return to photospheric temperatures via radiative losses. To model *these* processes, it is necessary to solve the time-dependent equation of motion (7) simultaneously with appropriate equations describing mass and energy conservation. This amounts to simulating ‘quasi-1D’ hydrodynamical flow along rigid magnetic flux tubes, with the cross-sectional area of the tubes varying in inverse proportion to the field strength.

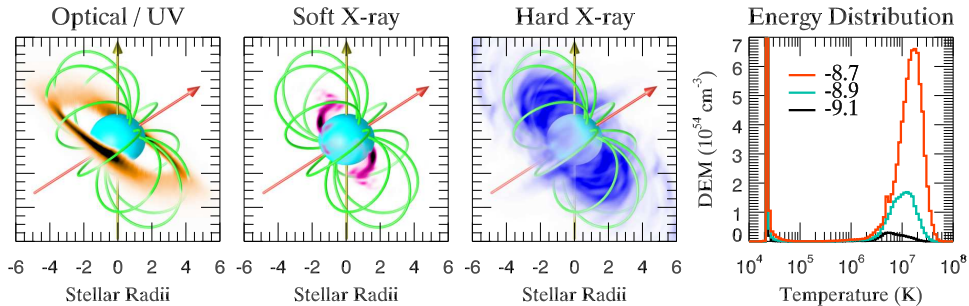


Figure 4. Renderings of an RFHD simulation of the magnetosphere of σ Ori E, showing the distribution of plasma which radiates in the optical / UV ($T < 10^6$ K), soft X-rays (10^6 K $< T < 10^7$ K) and hard X-rays ($T > 10^7$ K). The right-hand panel plots the corresponding differential emission measure for three different assumed mass-loss rates (labeled by $\log_{10} \dot{M}$). Note how the X-ray emission becomes softer and rapidly weaker as \dot{M} is reduced.

Townsend et al. (2007) applied such a *rigid-field hydrodynamics* (RFHD) approach to model the temporal evolution of the magnetosphere around a star similar to σ Ori E. Piecing together simulations along 1,140 field lines (run in parallel on a computer cluster, since they are independent of each other), these authors built up a 3-D picture of the star’s circumstellar environment, spanning 20 Msec, at a fraction of the cost of an equivalent MHD calculation. Key findings are that the distribution of cooled, static plasma predicted by the RRM and A-RRM model is correct; and that the X-ray emission from the wind-collision shocks appears to be sufficient to explain the X-rays observed from some helium-strong stars (note that in the specific case of σ Ori E, more than half of the X-ray flux in fact originates from a low-mass companion; see the contribution from Véronique Petit, these proceedings).

More-recent work based on the RFHD approach has explored how X-ray emission depends on the assumed mass loss rate. Using a revised RFHD code which includes field-parallel heat conduction and improved coupling between hydrodynamical and thermal processes, Hill et al. (2011) demonstrated that both the hardness and the overall flux of the emission is *extremely* sensitive to \dot{M} (see Fig. 4). This suggests that X-ray observations can be leveraged to constrain mass-loss rates of magnetic B stars — something quite difficult to achieve using other diagnostics.

4. Open Questions

Rigid-field models have proven extremely useful in enriching our understanding of massive-star magnetospheres. However, a number of open questions remain. It’s still not clear what mechanism is responsible for emptying plasma from centrifugal magnetospheres, in order to balance the every-present filling by the wind. Townsend & Owocki (2005) originally proposed that a CM accumulates plasma until the centrifugal force on field lines overwhelms magnetic tension; at this point, the stressed field reconnects, spilling plasma out of the magnetosphere. The appeal of this *centrifugal breakout* hypothesis was that the consequent sudden release of magnetic energy could explain the X-ray flaring seen in σ Ori E (Groote & Schmitt 2004; Sanz-Forcada et al.

2004). However, although MHD simulations provide support for the mechanism (see ud-Doula et al. 2006), it now seems more likely that the flaring in σ Ori E comes from the star’s X-ray bright companion (see above).

Even more telling, the analysis in the appendix of Townsend & Owocki (2005) argues that the total mass contained in a CM moderated by centrifugal breakout should approach the asymptotic value

$$M_\infty \approx 10^{-8} M_\odot \frac{B_3^2 R_{12}^2 W^{4/3}}{g_4}, \quad (13)$$

where B_3 is the stellar surface field strength in units of 10^3 G, R_{12} the stellar radius in 10^{12} cm, and g_4 the surface gravity in 10^4 cm s^{-2} (note the absence of the mass-loss rate from this expression). For the parameters of the stars plotted in the CM domain of Fig. 1, the fractional term in this expression is of order unity, and so $M_\infty \sim 10^{-8} M_\odot$. This value, however, is orders of magnitude larger than the magnetospheric masses $\lesssim 10^{-11} M_\odot$ inferred from observations, meaning that centrifugal breakout cannot play any important role in magnetospheric mass loss.

Havnes & Goertz (1984) explored whether cross-field diffusion processes can serve as an alternative mass-loss channel. Their general finding was that these are too slow to be relevant; revisiting their calculations with more up-to-date magnetospheric parameters does not change this conclusion. Thus, a complete understanding of magnetospheric mass budgets still needs to be developed.

A related open question concerns what processes might *redistribute* plasma within a magnetosphere, leading to departures from the distribution predicted by the RRM and A-RRM models. Time-series observations of high-order Balmer absorption lines (Smith & Bohlender 2007) and linear polarization (see the contribution by Alex Carciofi) in σ Ori E, and of H α emission (Leone et al. 2010) in δ Ori C, are suggestive of such departures.

5. Summary

Whether a magnetic massive star harbors a magnetosphere — and if so, whether the magnetosphere is dynamical or centrifugal — depends on its location in the η_* - W plane. Dynamical magnetospheres are typically found in O-type stars because mass-loss rates are high; whereas centrifugal magnetospheres are more often found in B-type stars because, with the lower mass-loss rates, the Alfvén radius lies outside the Kepler radius. MHD simulation remains the best tool for simulating DMs, but rigid field models are proving very successful in modeling CMs.

Acknowledgments. This work has been supported by NSF grants AST-0908688 and AST-0904607, and NASA grant NNX12AC72G.

References

- Babel, J., & Montmerle, T. 1997a, ApJ, 485, L29
- 1997b, A&A, 323, 121
- Bohlender, D. A., Landstreet, J. D., Brown, D. N., & Thompson, I. B. 1987, ApJ, 323, 325
- Bohlender, D. A., Walker, G. A. H., & Bolton, C. T. 1991, JRASC, 85, 202
- Borra, E. F., & Landstreet, J. D. 1979, ApJ, 228, 809

- Borra, E. F., Landstreet, J. D., & Thompson, I. 1983, *ApJS*, 53, 151
- Bouret, J.-C., Donati, J.-F., Martins, F., Escolano, C., Marcolino, W., Lanz, T., & Howarth, I. D. 2008, *MNRAS*, 389, 75
- Castor, J. I., Abbott, D. C., & Klein, R. I. 1975, *ApJ*, 195, 157
- Donati, J.-F., Babel, J., Harries, T. J., Howarth, I. D., Petit, P., & Semel, M. 2002, *MNRAS*, 333, 55
- Donati, J.-F., Howarth, I. D., Jardine, M. M., Petit, P., Catala, C., Landstreet, J. D., Bouret, J.-C., Alecian, E., Barnes, J. R., Forveille, T., Paletou, F., & Manset, N. 2006, *MNRAS*, 370, 629
- Groote, D., & Hunger, K. 1976, *A&A*, 52, 303
- 1982, *A&A*, 116, 64
- Groote, D., & Schmitt, J. H. M. M. 2004, *A&A*, 418, 235
- Havnes, O., & Goertz, C. K. 1984, *A&A*, 138, 421
- Henrichs, H. F., de Jong, J. A., Donati, D.-F., Wade, G. A., Babel, J., Shorlin, S. L. S., Verdugo, E., Talavera, A., Catala, C., Veen, P. M., Nichols, J. S., & Kaper, L. 2000, in *Magnetic Fields of Chemically Peculiar and Related Stars*, edited by Y. V. Glagolevskij, & I. I. Romanyuk, 57
- Hesser, J. E., Ugarte, P. P., & Moreno, H. 1977, *ApJ*, 216, L31
- Hill, N. R., Townsend, R. H. D., Cohen, D. H., & Gagné, M. 2011, in *Proc. IAU Symposium 272: Active OB Stars: Structure, Evolution, Mass-Loss and Critical Limits*, edited by C. Neiner, G. Wade, G. Meynet, & G. Peters, 194
- Hunger, K. 1974, *A&A*, 32, 449
- Kochukhov, O., Lundin, A., Romanyuk, I., & Kudryavtsev, D. 2011, *ApJ*, 726, 24
- Krtićka, J., Kubát, J., & Groote, D. 2006, *A&A*, 460, 145
- Landstreet, J. D., & Borra, E. F. 1978, *ApJ*, 224, L5
- Leone, F., Bohlender, D. A., Bolton, C. T., Buemi, C., Catanzaro, G., Hill, G. M., & Stift, M. J. 2010, *MNRAS*, 401, 2739
- Michel, F. C., & Sturrock, P. A. 1974, *Plan. Space. Sci.*, 22, 1501
- Nakajima, R. 1985, *Ap&SS*, 116, 285
- Owocki, S. P., & ud-Doula, A. 2004, *ApJ*, 600, 1004
- Pedersen, H., & Thomsen, B. 1977, *A&AS*, 30, 11
- Preuss, O., Schüssler, M., Holzwarth, V., & Solanki, S. K. 2004, *A&A*, 417, 987
- Sanz-Forcada, J., Franciosini, E., & Pallavicini, R. 2004, *A&A*, 421, 715
- Shore, S. N., & Brown, D. N. 1990, *ApJ*, 365, 665
- Shore, S. N., Brown, D. N., Sonneborn, G., Landstreet, J. D., & Bohlender, D. A. 1990, *ApJ*, 348, 242
- Smith, M. A., & Bohlender, D. A. 2007, *A&A*, 475, 1027
- Sundqvist, J. O., ud-Doula, A., Owocki, S. P., Townsend, R. H. D., Howarth, I. D., & Wade, G. A. 2012, *MNRAS*, L433
- Townsend, R. H. D., & Owocki, S. P. 2005, *MNRAS*, 357, 251
- Townsend, R. H. D., Owocki, S. P., & Groote, D. 2005, *ApJ*, 630, L81
- Townsend, R. H. D., Owocki, S. P., & Ud-Doula, A. 2007, *MNRAS*, 382, 139
- ud-Doula, A., & Owocki, S. P. 2002, *ApJ*, 576, 413
- ud-Doula, A., Townsend, R. H. D., & Owocki, S. P. 2006, *ApJ*, 640, L191
- Wade, G. A., Howarth, I. D., Townsend, R. H. D., Grunhut, J. H., Shultz, M., Bouret, J.-C., Fullerton, A., Marcolino, W., Martins, F., Nazé, Y., Ud Doula, A., Walborn, N. R., & Donati, J.-F. 2011, *MNRAS*, 416, 3160
- Walborn, N. R. 1973, *IAU Circ.*, 2612
- 1974, *ApJ*, 191, L95